Lifetimes and Failure Mechanisms of W/Re Hairpin Filaments

Prepared by

K. T. LUEY
Chemistry and Physics Laboratory
Laboratory Operations

26 February 1991

APR 3 1991

Prepared for

SPACE SYSTEMS DIVISION
AIR FORCE SYSTEMS COMMAND
Los Angeles Air Force Base
P.O. Box 92960
Los Angeles, CA 90009-2960

Engineering and Technology Group
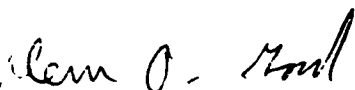
THE AEROSPACE CORPORATION
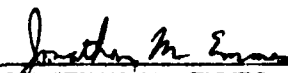El Segundo, California

91 4 22 047

This report was submitted by The Aerospace Corporation, El Segundo, CA 90245, under Contract No. F04701-88-C-0089 with the Space Systems Division, P.O. Box 92960, Los Angeles, CA 90009-2960. It was reviewed and approved for The Aerospace Corporation by J. M. Straus, Director, Chemistry and Physics Laboratory. Captain G. D. Good was the project officer for the Mission-Oriented Investigation and Experimentation (MOIE) program.

This report has been reviewed by the Public Affairs Office (PAS) and is releasable to the National Technical Information Service (NTIS). At NTIS, it will be available to the general public, including foreign nationals.

This technical report has been reviewed and is approved for publication. Publication of this report does not constitute Air Force approval of the report's findings or conclusions. It is published only for the exchange and stimulation of ideas.

GLENN D. GOOD, Capt, USAF
MOIE Project Officer
PL/WCO OL-AH

JONATHAN M. EMMES, Maj, USAF
MOIE Program Manager
PL/WCO OL-AH

REPORT DOCUMENTATION PAGE

1a. REPORT SECURITY CLASSIFICATION Unclassified	1b. RESTRICTIVE MARKINGS
2a. SECURITY CLASSIFICATION AUTHORITY	3. DISTRIBUTION/AVAILABILITY OF REPORT Approved for public release; distribution unlimited.
2b. DECLASSIFICATION/DOWNGRADING SCHEDULE	

4. PERFORMING ORGANIZATION REPORT NUMBER(S) TR-0090(5945-09)-1	5. MONITORING ORGANIZATION REPORT NUMBER(S) SSD-TR-91-06

6a. NAME OF PERFORMING ORGANIZATION The Aerospace Corporation Laboratory Operations	6b. OFFICE SYMBOL (If applicable)	7a. NAME OF MONITORING ORGANIZATION Space Systems Division
6c. ADDRESS (City, State, and ZIP Code) El Segundo, CA 90245-4691		7b. ADDRESS (City, State, and ZIP Code) Los Angeles Air Force Base Los Angeles, CA 90009-2960

8a. NAME OF FUNDING/SPONSORING ORGANIZATION	8b. OFFICE SYMBOL (If applicable)	9. PROCUREMENT INSTRUMENT IDENTIFICATION NUMBER F04701-88-C-0089

8c. ADDRESS (City, State, and ZIP Code)	10. SOURCE OF FUNDING NUMBERS			
	PROGRAM ELEMENT NO.	PROJECT NO.	TASK NO.	WORK UNIT ACCESSION NO.

11. TITLE (Include Security Classification)

Lifetimes and Failure Mechanisms of W/Re Hairpin Filaments

12. PERSONAL AUTHOR(S)
Luey, Kenneth T.

13a. TYPE OF REPORT	13b. TIME COVERED FROM _____ TO _____	14. DATE OF REPORT (Year, Month, Day) 1991 February 26	15. PAGE COUNT 29

16. SUPPLEMENTARY NOTATION.

17. COSATI CODES			18. SUBJECT TERMS (Continue on reverse if necessary and identify by block number)
FIELD	GROUP	SUB-GROUP	Tungsten Doped tungsten alloy filament failure
			Doped tungsten alloys Doped tungsten alloy recrystallization
			Doped tungsten

19. ABSTRACT (Continue on reverse if necessary and identify by block number)

A life test of tungsten hairpin filaments used in a high-reliability electron beam instrument has been carried out to improve knowledge of filament life and failure mechanisms as a function of temperature. These filaments are made of non-sag tungsten/3% rhenium (W/3% Re) wire. A steep reduction in filament life is observed at 2760 K which is not predicted by models which assume thermal evaporation as the principal failure mechanism. Failure analysis of the filaments shows that the sudden loss of life at 2760 K is the result of localized hot-spot formation caused by the accumulation of voids at grain boundaries. Examination of the crystal growth and growth rates indicates that the recrystallization temperature, T_{Rec}, occurs near 2760 K for the non-sag W/3% Re wire used in these filaments. This suggests that void accumulation acts as the principal life-limiting failure mechanism; spontaneous recrystallization at 2760 K increases the rate of void growth and causes a severe reduction of filament life.

20. DISTRIBUTION/AVAILABILITY OF ABSTRACT ☑ UNCLASSIFIED/UNLIMITED ☐ SAME AS RPT. ☐ DTIC USERS	21. ABSTRACT SECURITY CLASSIFICATION Unclassified
22a. NAME OF RESPONSIBLE INDIVIDUAL	22b. TELEPHONE (Include Area Code) 22c. OFFICE SYMBOL

DD FORM 1473, 84 MAR   83 APR edition may be used until exhausted.   SECURITY CLASSIFICATION OF THIS PAGE
All other editions are obsolete

UNCLASSIFIED

PREFACE

The author wishes to acknowledge useful and stimulating technical discussions with Drs. M. S. Leung, W. H. Kao, M. H. Hilton, and J. A. Wasynczuk. Mr. R. R. Seaver and Mr. N. A. Ives provided invaluable technical support.

1

CONTENTS

FIGURES

I. INTRODUCTION

High-reliability electron beam processing instruments can be severely impacted by filament failure in mid-operating cycle. In such instruments, it is desirable to have a precise knowledge of the filament life. With this knowledge, a filament near its end of life can be replaced prior to the start of an operating cycle when burnout is imminent. The need for filament life information is particularly vital for instruments using tungsten or tungsten alloy hairpin filaments because failure usually occurs catastrophically.

Traditionally, tungsten (W) filament life has been estimated using the empirical approach developed by Bloomer[1] and by Jones and Langmuir.[2] In this approach, end of life is due to wire thinning caused by thermal evaporation; filament life is thus a function of the W evaporation rate at a particular temperature. In Bloomer's experiments using straight, pure W wires, burnout occurs in times consistent with about 6% evaporative thinning over a broad range of test temperatures. Filament life prediction was therefore a matter of calculating the time for a 6% reduction of the wire diameter by evaporation.

In the development of long lived, incandescent lamp filaments, however, research has focused on the role of grain growth and grain boundary dynamics as the principal, life-limiting failure mechanism. Filament failure is thought to result from the growth of equiaxed grains and subsequent motion along the grain boundaries (sagging).[3-12] Recognition of these mechanisms led to the development of non-sag W wire which grew jagged, interlocking grains to inhibit sagging. A higher secondary recrystallization temperature, T_{Rec}, also resulted. Later, alloys of W and 3% to 20% rhenium (Re) were developed to further control grain growth and to improve ductility and resistance to vibration.

The failure mechanisms of non-sag doped wires of proprietary composition have been studied extensively and discussed most recently by Briant and Walter.[4] Dopants which are insoluble in W are dispersed during sintering and reside in the sintered ingot in the form of ellipsoidal

7

vacancies or voids. The ellipsoids break into strings of bubbles when the W is drawn into thin wires. These strings of bubbles are thought to be responsible for the growth of interlocking grains and the increased T_{Rec}. However, the bubbles have been seen to reaccumulate into large voids at grain boundaries which then contribute to the wire failure. Briant and Walter observed enhanced void nucleation as a function of temperature, mechanical stress, and oxygen environment in coiled, incandescent lamp filaments and straight wires, but did not carry their filament heating tests to failure. Earlier, Walter[5] performed life tests on doped W foils heated by alternating current. His tests strongly correlate failure sites with void nucleation at grain boundaries.

This report presents the results of life tests of W/3% Re hairpin filaments as a function of operating temperature using direct current. The filament lifetimes are discussed and compared with Bloomer's results[1] for the lives of straight, pure W wires and Briant and Walter's more recent results.[4]

II. EXPERIMENTAL PROCEDURE

A. SAMPLE SELECTION

The filaments under study are designated Type AR and are typically used in a scanning electron microscope (SEM). They are made of 0.006-in.-diameter wire which has been electrochemically etched to 0.005-in.-diameter at the tip. SEM micrographs of typical filaments as they appear when received from the vendor are shown in Figure 1. Growth of elongated grains in the tip resulted from a brief, low temperature anneal performed during manufacturing. Strings of bubbles can also be seen along the long axis of the crystals, which is typical of non-sag wire.

There is some variation in the shapes of the tips of different filaments; see Figure 2. Approximating the filament tip by a circular arc, the filaments shown in Figure 2 can be seen to have various radii of curvature, as indicated. To ensure uniformity of the samples, each filament was first inspected in an SEM, and only filaments having a radius of curvature less than 0.006 in. were selected for life testing. This approach was taken because it was assumed in this study that a tightly bent tip would be more effective in concentrating heat and would therefore better approximate a point source of electrons.

B. LIFE TEST ARRANGEMENT AND PROCEDURE

A schematic diagram of the experimental setup is shown in Figure 3. The filaments are heated in a stainless steel vacuum chamber at a maximum pressure of 1×10^{-7} Torr. Power is supplied by Sorensen-regulated dc power supplies in a constant voltage mode (current changes as filament resistance changes). The filament voltage is monitored inside the vacuum chamber at the filament posts, using the remote sense capability of the power supply. The filament current is determined by measuring the voltage across a 1.0 ohm ($\pm 1\%$) sensing resistor in series with the filament. The filament voltage, current, and operating time are logged by a micro-computer.
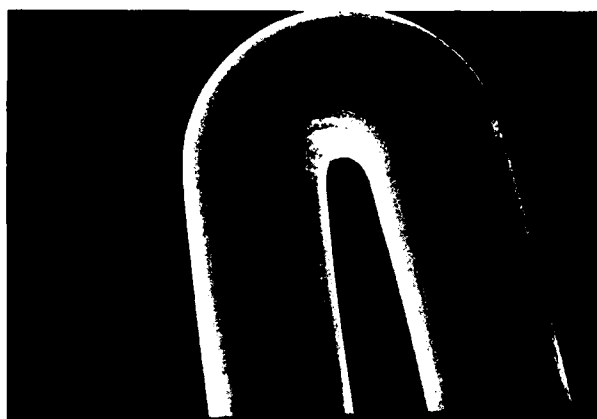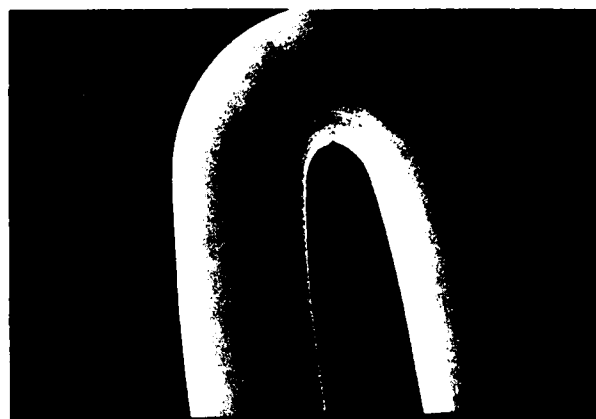
9

(a)

200 μm

(b)

100 μm

Fig. 1. Type AR filament as received from vendor. (a) Elongated
grain structure. (b) Rows of bubbles rise to surface
during crystal growth.

(a)

(b)

(c)

200 μm

(d)

Fig. 2. Scanning electron micrographs of Type AR tungsten
filaments. Radius of curvature: (a) 0.0055 in.,
(b) 0.0059 in., (c) 0.0065 in., (d) 0.007 in.
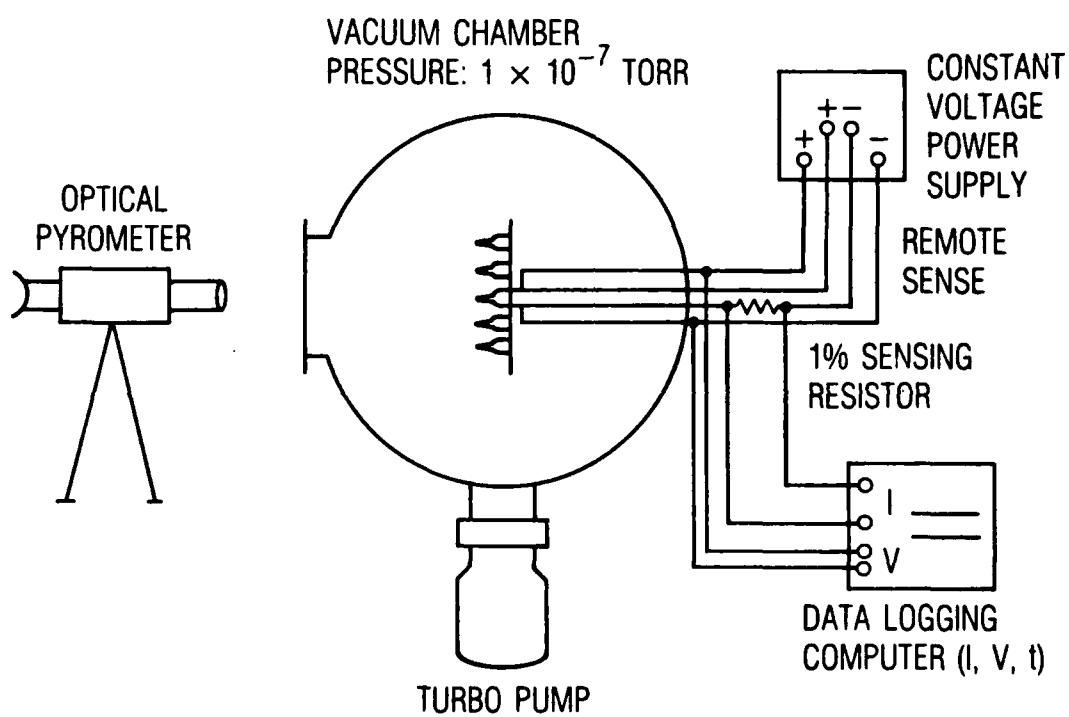
VACUUM CHAMBER
PRESSURE: 1×10^{-7} TORR

OPTICAL
PYROMETER

CONSTANT
VOLTAGE
POWER
SUPPLY

+ −
+ −

REMOTE
SENSE

1% SENSING
RESISTOR

I

V

DATA LOGGING
COMPUTER (I, V, t)

TURBO PUMP

Fig. 3.   Schematic of experimental setup.

A Pyro Micro-Optical disappearing filament pyrometer is used to measure the filament radiance temperatures, T_R, at 0.65 μm. The true temperatures in Kelvin, T_{True}, are obtained using Wien's law:

$$T_{True} = \frac{C_2 T_R}{C_2 + \lambda T_R \ln\epsilon} \qquad (1)$$

where

$$\lambda = 0.65 \text{ μm}$$
$$C_2 = ch/k = 1.44 \times 10^4 \text{ μ-K}$$

ϵ is the emissivity of tungsten at 0.65 μm, and T_R and T_{True} are in degrees K. In previous studies, $\epsilon = 0.46$ for clean, pure W;[14] however, the appearance of the filaments following heating, as will be shown, suggests that some change in ϵ occurs as the filaments age.

In their work, Briant and Walter fully recrystallized their filaments and wires prior to testing. For straight wires, this was done by heating for 1 h at 2673 K. As this procedure is not likely to be carried out in a typical electron beam instrument, the hairpin filaments tested here simply had their temperatures turned up slowly over the course of 2 to 4 h, as would be done with a new filament in a typical electron beam instrument in order to maintain a high vacuum. The actual heating rate maintained a vacuum level better than 1×10^{-6} Torr. Additional oxygen was not added to the vacuum, and no mechanical stresses were applied to these filaments, as was done by Briant and Walter.

III. RESULTS AND DISCUSSION

A. LIFE TEST RESULTS AND FAILURE ANALYSIS

Filament lives as a function of operating temperature are shown in Figure 4 for three distinct regions: (a) a low temperature region in which the filament temperatures are initially set at 2640 K or lower; (b) a transitional region with initial filament temperatures at 2760 K; and (c) a high temperature region where filaments are initially set at 2880 K or higher. The most striking aspect of these data is the abrupt loss of life in a narrow temperature range near the transitional region at 2760 K. In addition, the lives are significantly more scattered in the transitional region, while the lives are quite reproducible in the high and low temperature regions.

The dashed line in Figure 4 shows the predicted lives for ideal, 0.005-in.-diameter W wires using Bloomer's approach. Agreement with the measured lives of Type AR filaments appears to be good in the transitional region, but the wide scatter in the life there shows that a precise life prediction cannot be made in that temperature range. Bloomer's approach predicts lives that are too low in both the high and low temperature regions. Deviation from the life test results is greatest in the low temperature region, where only 300 h are predicted compared to the 1000 h observed in the life test.

The temperature behavior of the filaments also does not follow Bloomer's prediction for a constant voltage test, as pointed out by Wilson[15] in discussing his constant-current filament tests. Bloomer predicts that thinning of the wire causes a decrease in current and temperature. At 2640 K, Bloomer predicts a temperature decrease of 30 K for 6% thinning, while at 2760 K, the decrease is 36 K. The life test data here show that the current does decrease as the test progresses, but the filament temperature increases by 100 to 200 K, as seen in Figure 5. In the low and transitional temperature regions, the filament temperature remains constant for approximately the first half of the total life before the temperature begins to rise. In the high temperature region, the temperature increase begins within the first few hours of operation. Similar behavior, using alternating current, was observed by Walter.[5]
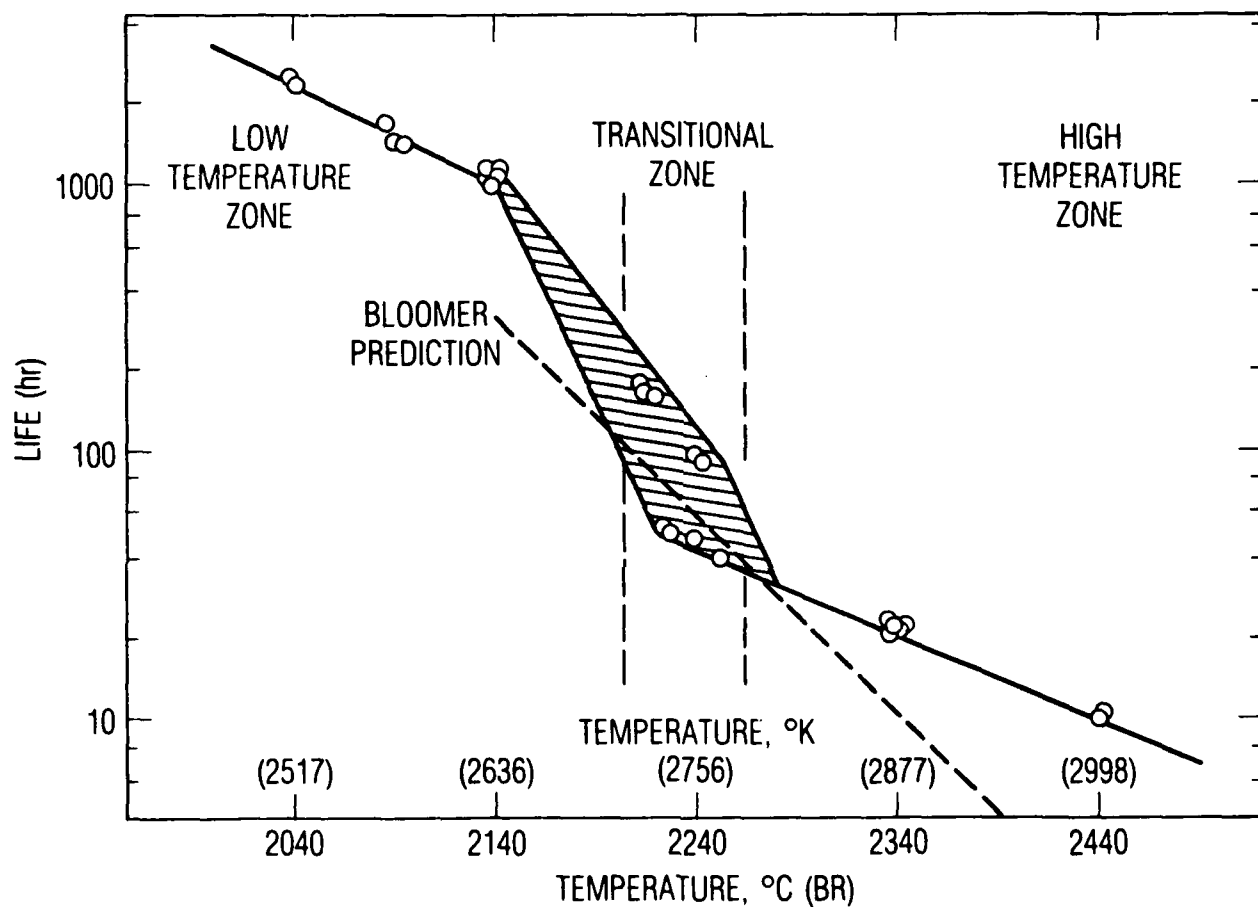
Fig. 4. Life test results of Type AR filaments. Dashed line is calculated life using Bloomer's approach.
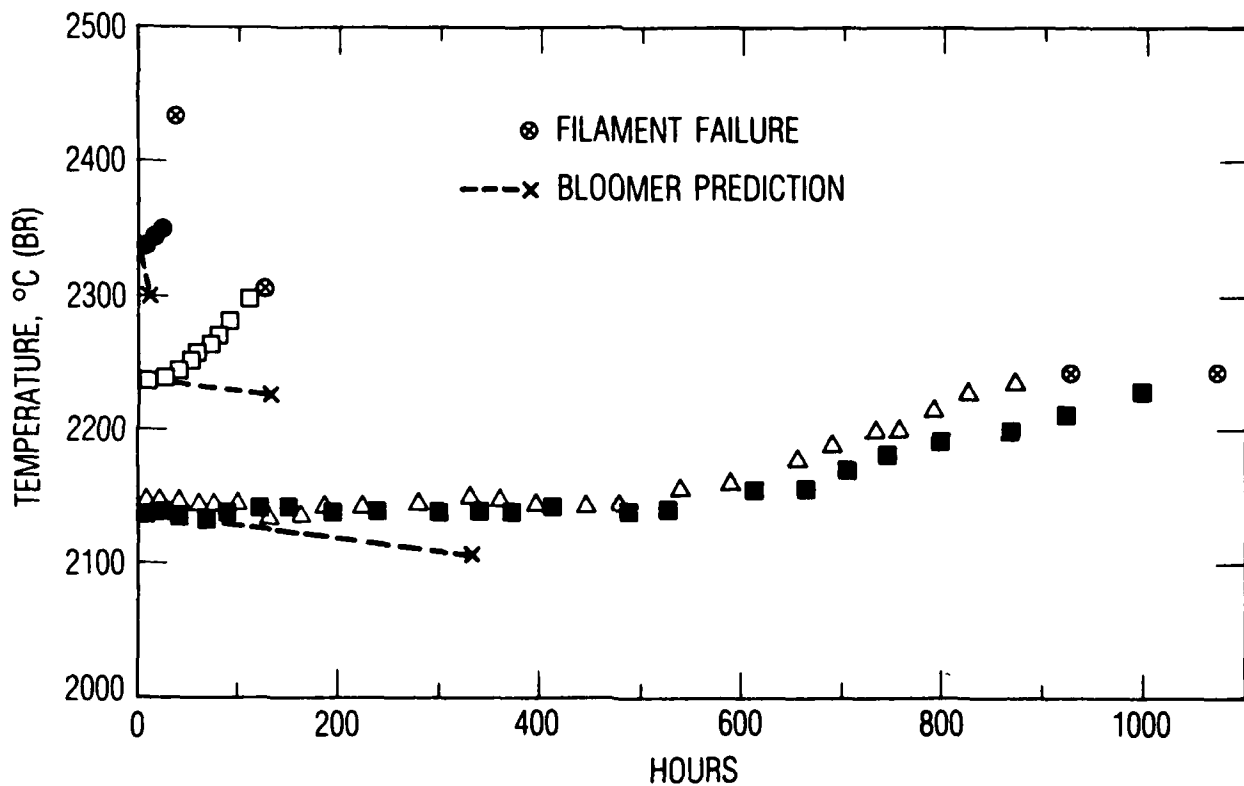
Fig. 5. Filament temperature versus hours of constant voltage test.
Dashed line is temperature behavior according to Bloomer's
result.

The temperature increase is not caused by an increase in ϵ. A change of ϵ from 0.46 to 1.0 is required to account for a 200 K increase in the temperature measurements in the range near 2700 K. Quinn[14] has examined increases in ϵ as a function of grain boundary faceting and concludes that ϵ changes by only 3% to 5% as grains grow to diameters of 50 to 100 µm. Most importantly, highly faceted filaments operated at 2640 K increase in temperature by the same amount as the much smoother filaments operated at 2880 K. Thus, increases in ϵ cannot be responsible for the temperature increase.

The failed filaments were examined in an SEM. Micrographs of failed filaments from each temperature region are shown in Figure 6. All of the filaments failed at the side of the filament just below the emitting tip and have a resolidified ball of melted tungsten on each end of the failed wire. The increasing filament temperature has reached the melting point of W, and burnout has occurred because the wire has melted in a localized region to the side of the tip.

The appearance of the failed filaments does not support a model of failure by 6% evaporative thinning. Figure 7 shows the filament failure sites at higher magnification to illustrate the differences in the length of the failure zone gap, the diameter of the resolidified melt, and the diameter of the wire just outside the failure zone. The dimensions of the failure site are different in each temperature region. At low temperatures, Figure 7(a) shows that only a small volume of wire reaches the W melting point. The resolidified melt is 15 µm in diameter, and the gap between the wire ends is 20 µm. There is also a slight offset between the two ends, indicating transverse motion of the wire occurs during failure. In contrast, the filament operated at high temperature shown in Figure 7(c) has much larger volumes of melt separated by a wider gap. The wire just behind the melt is also of larger diameter than for filaments operated at low temperature.

In summary, the life test results disagree with Bloomer[1] and Jones and Langmuir[2] in two respects. First, as discussed above, filaments operated at different temperatures do not suffer the same amount of material loss prior to failure. Bloomer's study concludes that filaments fail following

18

(a)

(b)

(c)
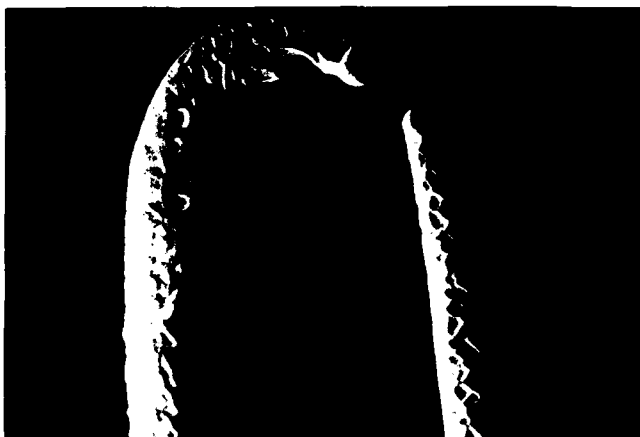
100 μm

Fig. 6. Type AR filaments
following failure.
Initial temperature/life:
(a) 2640 K/1052 h
(b) 2760 K/105 h
(c) 2880 K/23 h

(a)

(b)

(c)

Fig. 7. Filament failure sites.
Initial temperature:
(a) 2640 K
(b) 2760 K
(c) 2880 K

50 μm

the criterion of 6 to 10% reduction of diameter by evaporation, regardless of the temperature. Secondly, the gradual cooling predicted for a constant-voltage life test does not occur here. This finding suggests that the usual failure model using uniform wire thinning by thermal evaporation is not accurate for non-sag W and W/Re wires.

B. RECRYSTALLIZATION TEMPERATURES AND EFFECTS

The abrupt decrease in life without the concomitant material loss suggests the onset of a new or additional failure mechanism at about 2760 K. A new failure mode above 2700 K is consistent with the properties of non-sag W and W/Re wire reported in the literature. In stress tests, an abrupt decrease in the tensile strength is observed at about 2650 K in W wire doped with potassium (K).[13] T_{Rec} for K-doped W wire has also been observed to be a function of wire diameter[10] and occurs at approximately 2700 K for diameters of about 0.006 in. In K-doped W/3% Re alloy, T_{Rec} is further elevated by as much as 200 to 300 K in some reports. Although Briant and Walter do not disclose the composition of the wire used in their study, their wires are reported as fully recrystallized after heating for 1 h at 2573 K. It is therefore expected that T_{Rec} seen in the W/3% Re filaments studied here should be higher than that reported in the literature for K-doped W. The analyses discussed below provide greater detail on the nature of the grain growth and the temperature at which recrystallization begins.

A cross-sectional micrograph of an as-received Type AR filament is shown in Figure 8. Each leg exhibits the fine-grained character of the swaged wire, while much larger grains have grown in the curved tip. These grains in the tip have grown as a result of a brief low-temperature heating cycle included in the filament manufacturing procedure. Bending the wire introduces cold working that decreases T_{Rec} in the tip without affecting T_{Rec} in the legs. During heating at a temperature below T_{Rec}, the legs maintain their fine-grained appearance, while large crystals grow readily in the tip. At greater magnification, a boundary is seen between the large crystal grains in the tip and the fine-grained wire in the legs, see Figure 8(b). This boundary coincides with the eventual burnout site shown in Figure 6. Some as-received filaments display a crack on the underside

21

(a)

200 μm

(b)
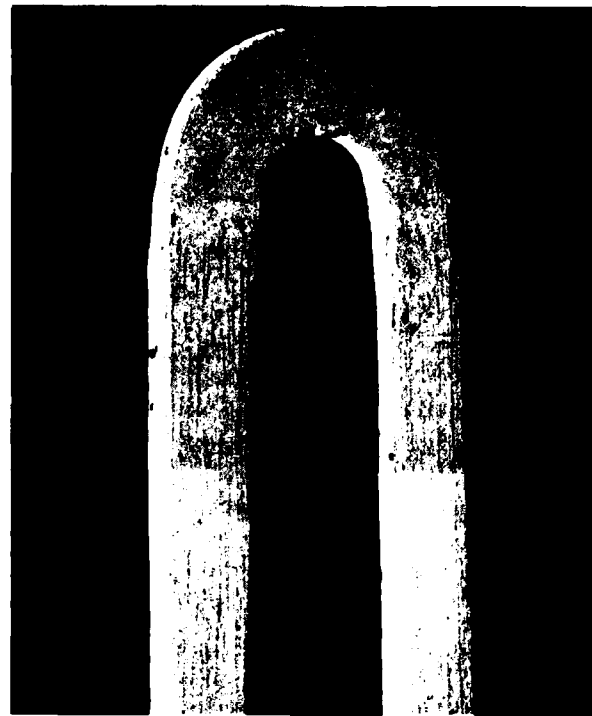
100μm

Fig. 8. (a) Cross sectional view of Type AR filament as received
from vendor. (b) Boundary between fine-grained, swaged
wire and large grains in tip.

22

of the tip, also shown in Figure 8(b). However, in all cases but one, burnout occurs to the side of the tip whether the filament is cracked or not.

A separate study was conducted to examine filament grain structure very near the end of life, particularly near the known burnout site. As part of this study, several filaments were heated and then removed near their known lifetimes, usually after the filament temperatures had risen about 100 to 150 K. Two examples of filaments from this study are discussed below.

A cross-sectioned filament heated for 900 h, starting at 2640 K and ending at 2840 K, is shown in Figure 9. The small grains in the legs have converted into much larger crystals as a result of the prolonged heating. (The apparent thinness of the right-hand leg is caused by the filament not lying flat in the polishing block and not by a greater degree of thermal evaporation.) Figure 9 also shows that the grains cannot extend from the leg into the tightly bent tip. As a result, a boundary forms where the elongated grains of the legs meet with the preexisting grains in the tip.

Most importantly, Figure 9(b) shows that a void has collected at the boundary between these grains, exactly where filaments are seen to eventually fail. The void is about 25)m in diameter (and possibly larger, since the cross sectioning might not be revealing the maximum diameter of the void) and causes a hot spot at the grain boundary. The formation of the void at this grain boundary is consistent with several studies on the growth of voids in doped W. Briant and Walter have shown the effects of stress, creep, and oxygen environment on void nucleation at grain boundaries. In this study, the hairpin filaments have been annealed during manufacture and are heated for longer times during life testing. There is no appreciable added stress during the life test, nor is there a substantial level of oxygen.

A second filament, shown in Figure 10, was heated for 20 h starting at a temperature of 2880 K and ending at 3000 K. In this case, the legs have grown completely into single crystals. Only two small crystals are seen on the insides of the legs just below the tip instead of the much larger
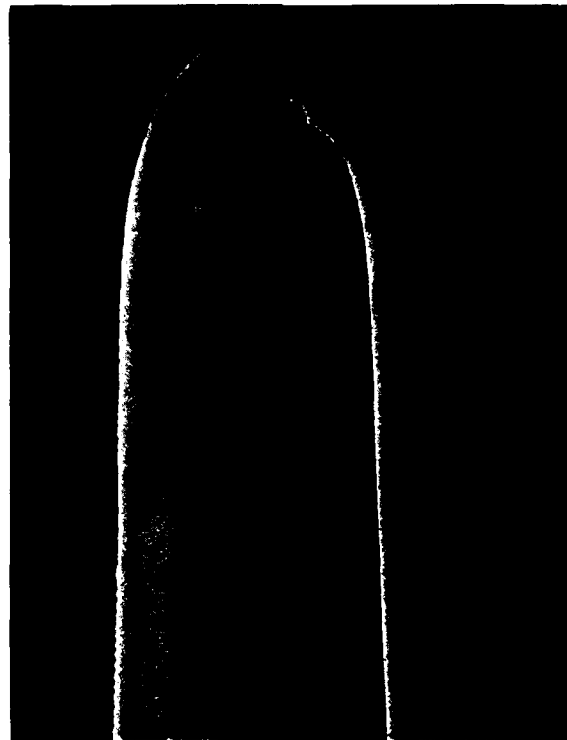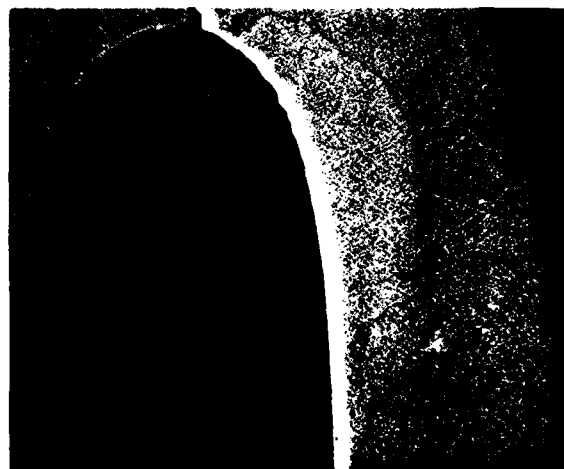
23

(a)

⊢——⊣
100 μm

(b)
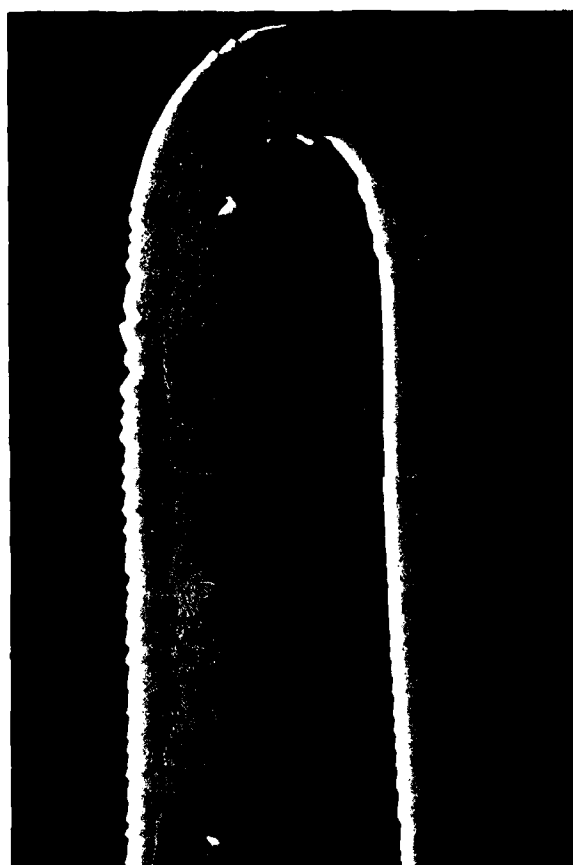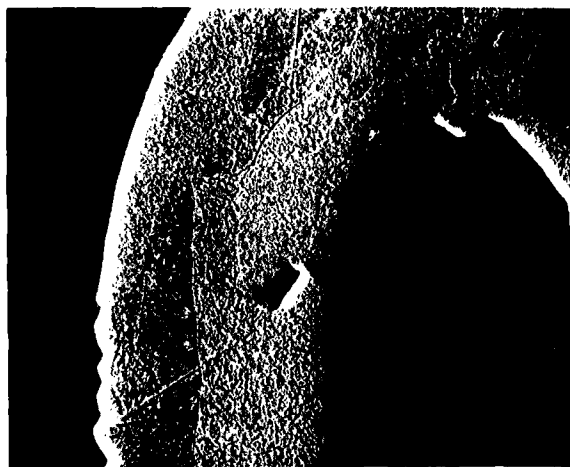
⊢——⊣
50 μm

Fig. 9. (a) Cross sectional view of Type AR filament heated for 800 h at 2640 K. (b) Formation of void at grain boundary just below tip.

24

(a)

100 μm

(b)

50 μm

Fig. 10. (a) Cross sectional view of Type AR filament heated for
18 h at 2880 K. (b) Grain boundary below tip.

crystals seen in Figure 9. Recrystallization is clearly much more rapid at 2880 K. These results show that recrystallization rates are quite different above and below the temperature at which filament life is seen to abruptly decrease.

Note that while a distinct grain boundary is observed in Figure 10, no void is seen there despite the temperature increase. One possibility is that the void has nucleated at the top of the filament where the crack is located. This might be possible because the filament in Figure 10 is not as tightly bent as the filament shown in Figure 9. The filament shown in Figure 10 was not chosen as a life test sample because of its large tip radius. Because of both the increased test temperature and the large tip radius, much larger crystals can be seen to have grown in the tip, compared to those grown at lower temperature in a filament with a smaller tip radius. In a preliminary test of filaments having large tip radii, one of three filaments tested at 2880 K was observed to fail at the top of the filament tip.

To more precisely specify T_{Rec}, two filaments were heated for 18 h at 2640 K and 2760 K. Little change of temperature was observed during this test. At 2640 K, the filament begins to develop a faceted, crystalline appearance; see Figure 11(a). Reexamination of Figure 6 shows that the rough, faceted appearance is maintained and that the depth and length of the facets increase after 1000 h. In contrast, the filament shown in Figure 11(b), heated at 2760 K, also for 18 h, displays larger, smoother grains. These results indicate that the difference in crystal morphology seen in Figure 11 is purely a function of temperature and that filament recrystallization begins in a narrow temperature range near 2760 K.

The reason for the widely dispersed filament life at 2760 K is not well understood and requires more detailed study. The most probable causes are the varying amount of cold work in the tip and the extent of the low temperature anneal during manufacturing. The filaments are bent by hand using special tools, and the various amounts of cold working will cause different changes in T_{Rec} in the tip region. In addition, the annealing time and temperature can vary significantly for different filaments. Annealing variations can result in different degrees of crystal growth in

(a)
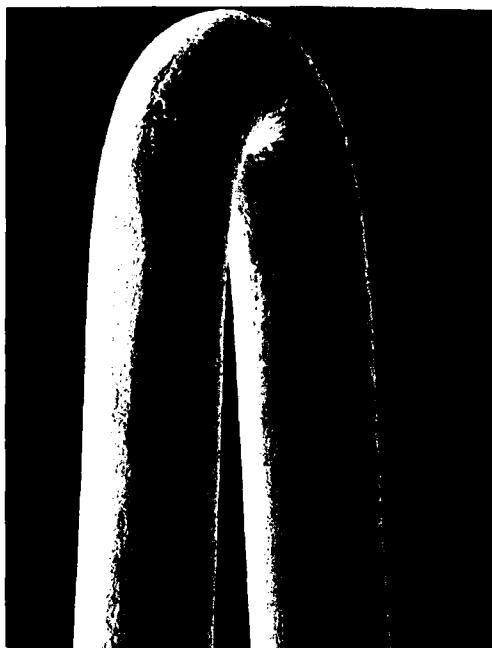
(b)   ⊢——————⊣
      100 μm

Fig. 11. (a) Type AR filament heated for 18 h at (a) 2640 K (note
         maintenance of swaged wire appearance in legs), and
         (b) 2760 K (growth of large, smooth crystals in legs
         is evident).

27

the tip and legs. These variations most likely do not have a significant impact on life well above T_{Rec} because recrystallization proceeds so rapidly. Similarly, well below T_{Rec}, recrystallization proceeds much more slowly and small variations in the manufacturing anneal are not likely to impact life significantly.

A model for the failure of Type AR filaments which includes recrystallization effects explains well the results from this life test. Recrystallization occurs spontaneously at temperatures at or above T_{Rec}. Spontaneous recrystallization increases the rate of bubble migration toward the grain boundary just below the emitting tip. The bubble migration is driven by the thermal gradient between the emitting tip and the filament leg.[4] The bubbles coalesce at the grain boundary, forming a hot spot and producing rapid failure. At temperatures below T_{Rec}, recrystallization and bubble migration proceed more slowly and significantly longer filament lives are observed. Short term tests in a small temperature range indicate that T_{Rec} for non-sag W/3% Re filaments lies near 2760 K. This model is consistent with Briant and Walter. Their studies begin with fully recrystallized wires and, thus, conclude that large voids nucleate at bubbles already present at the grain boundaries. The fully recrystallized condition is not present in a new hairpin filament and proceeds to recrystallize slowly if operated below T_{Rec} or more rapidly if operated above T_{Rec}.

IV. CONCLUSIONS

The lifetimes of non-sag W/3% Re hairpin filaments have been studied as a function of operating temperature. The results show an abrupt decrease in life at temperatures at or above 2760 K. An abrupt, precipitous loss of life at this temperature is not predicted by life prediction models which assume thermal evaporation and thinning as the principal, life-limiting failure mechanism. In addition, Bloomer's evaporative thinning model[1] for straight, pure W wires in constant-voltage tests predicts that the filament temperature decreases by about 30 to 40 K with time. In this test of hairpin filaments at constant voltage, however, an increase of up to 200 K is observed prior to failure.

SEM failure analyses indicate that the sudden loss of life is caused by recrystallization, which occurs spontaneously at about 2760 K. Recrystallization occurs more slowly as the filament is operated at lower temperatures. Recrystallization brings about formation of voids at the grain boundary, which forms just below the emitting tip between the straight wire of the filament legs and the curved emitting tip. This grain boundary acts as the failure site in tightly bent filaments because the voids collect there and cannot migrate further into the tip.

REFERENCES

1. R. N. Bloomer, Proc. Inst. Elec. Eng., 1957, 104 (B), pp. 153-157.

2. H. A. Jones and I. Langmuir, General Electric Review, 1927, 30, pp. 310-319.

3. S. Dushman, General Electric Review, 1915, 18, pp. 156-167.

4. C. L. Briant and J. L. Walter, Acta Metall.,1988, 30 (9), pp. 2503-2514; J. L. Walter and C. L. Briant. J. Mater. Res., September 1990, 5 (9), pp. 2004-2022.

5. J. L. Walter, J. Appl. Phys., 1986, 60 (9), pp. 3343-3355.

6. D. M. Moon and R. C. Koo, Metall. Trans. 1971, 2, pp. 2115-2122.

7. S. W. H. Yih and C. T. Wang, Tungsten: Sources, Metallurgy, Properties, and Applications, Plenum Press, New York, 1979, pp. 216-219.

8. R. P. Simpson, G. J. Dooley, III, and T. W. Haas, Metall. Trans, 1974, 5, pp. 585-591.

9. S. Garbe and S. Hanloh, Philips J. Res., 1983, 38, pp. 248-262.

10. O. Horacsek, Z. Metallkd.,1974, 65 (4), pp. 318-323.

11. A. Berghezan and A. Fourdeux, Planseeberichte für Pulvermetallurgie, 1974, 22, pp. 264-284.

12. R. Raj and G. W. King, Metall. Trans A, 1978, 9A, pp. 941-946

13. K. C. Thompson Russell, Planseeberichte für Pulvermetallurgie, 1974, 22, pp. 155-164.

14. Temperature, T. J. Quinn, Academic Press, London, 1983, pp. 284-367.

15. A. D. Wilson, J. Appl. Phys., 1969, 40 (4), pp. 1956-1964.

LABORATORY OPERATIONS

The Aerospace Corporation functions as an "architect-engineer" for national security projects, specializing in advanced military space systems. Providing research support, the corporation's Laboratory Operations conducts experimental and theoretical investigations that focus on the application of scientific and technical advances to such systems. Vital to the success of these investigations is the technical staff's wide-ranging expertise and its ability to stay current with new developments. This expertise is enhanced by a research program aimed at dealing with the many problems associated with rapidly evolving space systems. Contributing their capabilities to the research effort are these individual laboratories:

Aerophysics Laboratory: Launch vehicle and reentry fluid mechanics, heat transfer and flight dynamics; chemical and electric propulsion, propellant chemistry, chemical dynamics, environmental chemistry, trace detection; spacecraft structural mechanics, contamination, thermal and structural control; high temperature thermomechanics, gas kinetics and radiation; cw and pulsed chemical and excimer laser development, including chemical kinetics, spectroscopy, optical resonators, beam control, atmospheric propagation, laser effects and countermeasures.

Chemistry and Physics Laboratory: Atmospheric chemical reactions, atmospheric optics, light scattering, state-specific chemical reactions and radiative signatures of missile plumes, sensor out-of-field-of-view rejection, applied laser spectroscopy, laser chemistry, laser optoelectronics, solar cell physics, battery electrochemistry, space vacuum and radiation effects on materials, lubrication and surface phenomena, thermionic emission, photosensitive materials and detectors, atomic frequency standards, and environmental chemistry.

Electronics Research Laboratory: Microelectronics, solid-state device physics, compound semiconductors, radiation hardening; electro-optics, quantum electronics, solid-state lasers, optical propagation and communications; microwave semiconductor devices, microwave/millimeter wave measurements, diagnostics and radiometry, microwave/millimeter wave thermionic devices; atomic time and frequency standards; antennas, rf systems, electromagnetic propagation phenomena, space communication systems.

Materials Sciences Laboratory: Development of new materials: metals, alloys, ceramics, polymers and their composites, and new forms of carbon; nondestructive evaluation, component failure analysis and reliability; fracture mechanics and stress corrosion; analysis and evaluation of materials at cryogenic and elevated temperatures as well as in space and enemy-induced environments.

Space Sciences Laboratory: Magnetospheric, auroral and cosmic ray physics, wave-particle interactions, magnetospheric plasma waves; atmospheric and ionospheric physics, density and composition of the upper atmosphere, remote sensing using atmospheric radiation; solar physics, infrared astronomy, infrared signature analysis; effects of solar activity, magnetic storms and nuclear explosions on the earth's atmosphere, ionosphere and magnetosphere; effects of electromagnetic and particulate radiations on space systems; space instrumentation.